NASA CR 182141

Solar Dynamic Heat Rejection Technology
Task 2 Final Report
Heat Pipe Radiator Development

Mark League, Joe Alario
Grumman Space Systems Division

May 1988

Prepared for the
Lewis Research Center
Under Grant NAS3-24665

National Aeronautics and
Space Administration

NASA CR 182141

Solar Dynamic Heat Rejection Technology
Task 2 Final Report
Heat Pipe Radiator Development

Mark League, Joe Alario
Grumman Space Systems Division

May 1988

Prepared for the
Lewis Research Center
Under Grant NAS3-24665

National Aeronautics and
Space Administration

6098-88

CONTENTS

ILLUSTRATIONS

ILLUSTRATIONS (contd)

SUMMARY

This report covers the design, fabrication, and test of several dual-slot heat pipe engineering development units. This heat pipe design has been identified as a critical component in the development of a high capacity radiator system for the Space Station solar dynamic power system because its envelope structure can be fabricated from a variety of different materials. The following dual-slot heat pipes were fabricated and tested to establish proof of concept:

- 6-ft aluminum heat pipes with flat baffle assemblies (S/N 201 and 203)
- 6-ft aluminum heat pipe, S/N 203, reconfigured with a D-baffle assembly (S/N 203-D)
- 20-ft aluminum heat pipe with a T-baffle assembly (S/N 210)
- Four-leg evaporator, 20-ft aluminum heat pipe with a flat baffle assembly (S/N 301)

The actual thermal performance of S/N 201 and 203 was better than predicted. Test results indicate that because of their short length and the low heat fluxes applied during testing, these test articles may be capable of transporting heat while in an unstable, partial dryout condition.

The other three test articles experienced problems during startup of operation. Large temperature oscillations occurred in the evaporator sections of S/N 203-D and 210, which caused the pipes to dry out at operating conditions well below their predicted performance. Five test runs on S/N 210 did not experience these problems and they matched very close to the predictions. The cause of the temperature oscillations is thought to be boiling in the liquid channel of the evaporator. No test runs could be completed on S/N 301 because the pipe never reached a steady-state temperature condition after startup. The vapor channel of the condenser appears to be blocked by liquid that is not being drawn into the liquid channel. This slowly starves the evaporator of liquid and causes the observed temperature creep.

The methodology for fabricating stainless steel dual-slot heat pipes was also studied by performing a tool life test with different single point cutters. Three different geometries were tested with two different types of carbide. The cutter design that produced the longest length of cut was then tested with two different coatings. The longest length of grooves cut on the outside of a 2-in. stainless

steel bar was 30-in. of grooves in 0.75-in. OD tubing, which is adequate for making a stainless steel/methanol heat pipe. Unfortunately, our attempt at cutting grooves in tubing were unsuccessful because the tubes were out of round. Reaming the tubes before cutting grooves should produce better results, but we were unable to accomplish this task due to lack of funds.

Although, the dual-slot heat pipe has demonstrated the potential to meet the requirements for a high capacity radiator system, uncertainties with the design still exist. The startup difficulties with the aluminum test articles must be solved, and a stainless steel/methanol heat pipe should be built and tested before the dual-slot heat pipe can become an acceptable, low-risk design for a wide variety of heat rejection applications. We recommend that the test article S/N 301 be retested with a new condenser leg, using a screen wick covered flat baffle assembly. The screen wick offers another path for condensed liquid in the vapor channel to wick to the liquid channel, or conversely, for trapped vapor in the liquid channel to vent to the vapor channel. This design should solve both of the startup problems identified above. We also recommend that when a stainless steel heat pipe is built, the tubes be reamed before being grooved, and a titanium nitride coating be used on the single point cutters.

INTRODUCTION

The Space Station is projected to require approximately 300 kW_e in its final, full-growth configuration. This power is to be generated by a combination of photovoltaic panels and solar dynamic power modules. Electricity is generated in the modules by means of a thermodynamic cycle. The magnitude of the thermal energy generated as waste heat by the thermodynamic cycle is typically several times the magnitude of the electrical energy produced; thus, the heat rejection system is a critical part of the modules.

Grumman Space Systems was awarded an advanced development contract to study the heat rejection technology required to meet the needs of the Space Station solar dynamic electric power system. Concept development, design, and analysis of waste heat transport loop/radiator systems for both the organic Rankine cycle (ORC) and the closed Brayton cycle (CBC) solar dynamic power systems were performed in Task 1 of this contract. The results of this tradeoff study are presented in Ref 1.

High capacity heat pipe radiator systems can meet the Space Station requirements of long life, high reliability, and low maintenance. The monogroove heat pipe, developed by Grumman for the Space Station central radiator system under contracts to NASA-Johnson Space Center (JSC) and a derivative of the monogroove known as the dual-slot heat pipe were both studied in Task 1. For the ORC solar dynamic heat rejection system, we recommended an aluminum/ammonia dual-slot heat pipe radiator design as the baseline configuration, with the aluminum/ammonia monogroove heat pipe radiator design as a backup. For the CBC solar dynamic heat rejection system, we recommended a stainless steel/methanol or titanium/methanol dual-slot heat pipe radiator system as the baseline configuration. Thus, the dual-slot heat pipe was identified in Task 1 as a critical technology requiring further development and evaluation. Since the completion of Task 1, it should be noted that NASA has selected the CBC solar dynamic power system to be used on the Space Station. This makes the development of the dual-slot heat pipe all the more critical since no other heat pipe radiator is designed to operate at the high operating temperatures of the CBC power system.

The scope of Task 2 was to design, fabricate, test, and evaluate the dual-slot heat pipe. The general approach in this development program was to start with

short aluminum heat pipes and progress to a longer aluminum, multi-leg evaporated aluminum heat pipe. Parallel to this effort, we developed the technology to fabricate a stainless steel dual-slot heat pipe. This staged approach was taken to gain an understanding of each of the many factors that determine heat pipe behavior. This report presents the results of that effort.

HIGH CAPACITY HEAT PIPE CONFIGURATIONS

Cross sections of the monogroove heat pipe and dual-slot heat pipe configurations are shown in Fig. 1. The monogroove heat pipe is constructed from an aluminum extrusion, which limits its use to fluids that are compatible with aluminum, such as ammonia. The dual-slot heat pipe consists of a circular tube with a baffle inside. If made of aluminum tubing, the dual-slot heat pipe is lower in weight than a monogroove heat pipe sized for the same performance. More important, it can be made from materials other than aluminum, so the dual-slot heat pipe design is not limited to use with fluids that are compatible with aluminum.

The primary distinguishing features of both configurations are the large longitudinal vapor and liquid channels and the fine circumferential grooves machined on the inner wall. Both types of heat pipes operate on the same principles. The circumferential grooves provide a capillary wicking action that transports the heat pipe working fluid from the liquid channel to the vapor channel in the heat pipe evaporator section by means of surface tension. Liquid evaporates at the walls of the vapor channel when heat is applied to the evaporator. The vapor flows axially in the vapor channel to the condenser section where it condenses on the vapor channel walls. In the condenser section, the circumferential grooves provide a flow

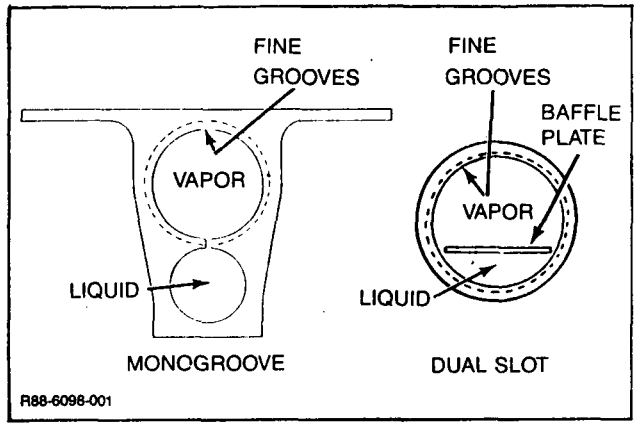

Figure 1 High Capacity Heat Pipe Cross Sections

path into the liquid channel for the condensate, and the cycle is completed when the liquid flows axially in the liquid channel to the evaporator.

The longitudinal pressure differential between the liquid and vapor channels is sustained by the meniscus at the "slots" that separate the liquid and vapor channels. In the monogroove configuration, the slot is an integral part of the heat pipe extrusion. In the dual-slot heat pipe, the slots are formed by the circumferential grooves at the two edges of the baffle (hence the term "dual slot"), provided the baffle is in contact with the wall. At any location at which the baffle does not touch the wall, the slot is formed by the grooves as well as the gaps between the baffle and the wall.

The high axial thermal transport capacity of these configurations is due to the large cross-sectional areas of the liquid and vapor channels (resulting in very low longitudinal pressure drops per unit length) and the small slot widths that support a high capillary pressure difference. The fine circumferential grooves provide high evaporation and condensation film coefficients.

HEAT PIPE PERFORMANCE PREDICTIONS

The thermal performance of both heat pipes is characterized by two differential pressure balances, shown in Fig. 2, that must be satisfied simultaneously. Equation 1 in Fig. 2 shows that the wall wick capillary pressure rise must offset

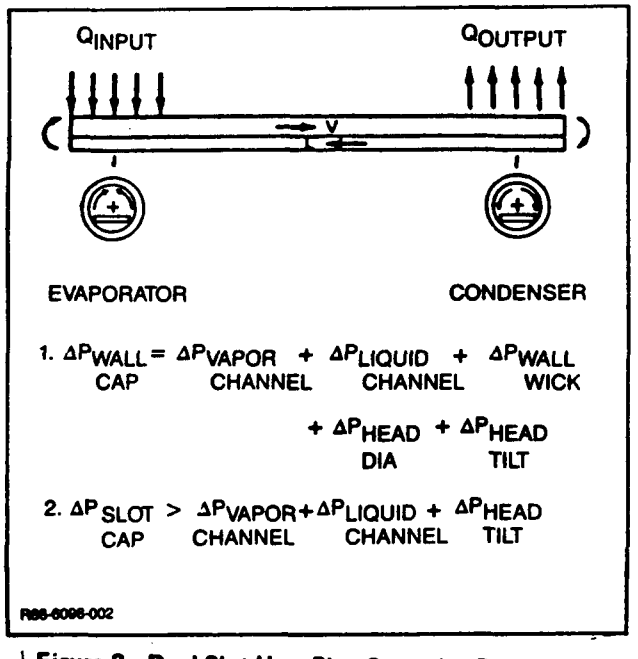

Figure 2 Dual-Slot Heat Pipe Operating Principles

the cumulative viscous pressure losses in the vapor channel, liquid channel, and circumferential wall grooves, plus the gravity head losses or gains associated with the height of the vapor channel and the tilt of the pipe (i.e., elevation difference between the evaporator and condenser sections). In addition, as indicated by Equation 2, the slots must develop enough capillary rise to overcome the longitudinal vapor and liquid viscous losses plus the gravity head loss or gain due to tilt. If either equation is not satisfied, the pipe will become unstable and cease to operate.

Grumman has developed two proprietary computer codes to calculate the thermal transport capacity of the monogroove and dual-slot heat pipes. By performing parametric studies, we can use the codes to optimize the designs of the two heat pipes. The computer code developed for the monogroove heat pipe has been validated by comparison with results from ground testing, with ammonia as the heat pipe working fluid (Ref 2, 3). The tests conducted in Task 2 and reported here are used to validate the code for the dual-slot heat pipe. Both codes were used in the Task 1 trade studies, which found that the dual-slot heat pipe offers a significant weight savings over a monogroove heat pipe of similar performance limits at the expense of being a higher technological risk.

FABRICATION OF ALUMINUM HEAT PIPES

Machining circumferential grooves in aluminum was accomplished in the development of the monogroove heat pipe and did not have to be repeated. The manufacturing procedures and tool fixtures needed only slight modifications to accommodate the dual-slot design. Standard 3/4-in. outside diameter, 0.062-in. wall, 6061-T6 aluminum tubing is first reamed to ensure the tube is true along its entire length. Next, grooves are cut into the inner wall of the tubes using single point cutters made of C-2 micrograin carbide. The same lathe fixture is used for both the reaming and grooving operations. The grooves are inspected using photomicrograph exposures of mounted samples taken from each end of the grooved tubes magnified 20 times.

The dimensions of each heat pipe fabricated for test are given in Table I. These dimensions are used by the computer code to create a map of the expected thermal performance of each heat pipe.

Three 6-ft heat pipes (S/N 201, 202, and 203) were built and tested first. Pipes 201 and 203 were used for thermal tests only. Pipe 202 was used strictly for

TABLE I DUAL-SLOT HEAT PIPE ALUMINUM TEST ARTICLE SPECIFICATIONS (in.)

Heat pipe no.	201	202	203	210	301
Overall length	71.5	73.8	72.0	240.0	240.0
No. evaporator legs	1	N/A	1	1	4
Evaporator length	22.0	N/A	22.0	48.0	24.0
Condenser length	22.0	N/A	24.0	60.0	60.0
Transport length	27.5	N/A	26.0	132.0	156.0
Outer diameter	0.75	0.75	0.71	0.75	0.75
Inner diameter	0.59	0.59	0.59	0.63	0.63
Baffle width	0.53	0.53	0.53	0.59	0.59
Circumferential grooves					
TPI	160	160	160	160	160
Depth	0.0042	0.0040	0.0032	0.0065	0.0045
Width (top)	0.0023	0.0028	0.0029	0.0025	0.0024
Effective slot width	0.0023	0.0030	0.0048	0.0040	0.0125

R88-6098-022

lift tests. The groove profile of the first three pipes varied slightly from each other; however, the next batch of grooved tubes was more consistent. The two grooved tubes used to build the 20-ft single-leg evaporator heat pipe (S/N 210) had identical groove profiles. The 2-ft evaporator legs for the multi-leg evaporator heat pipe (S/N 301) were made from solid 6061-T6 aluminum blocks. Of the eight legs built, three of the bores were not drilled true and were later lapped true with a silicon carbide lapping compound. Unfortunately, grooves could not be cut in these legs since some of the lapping compound became embedded in the aluminum wall and was breaking the single point cutters. The average measurements of the grooves in the remaining five legs are given in Table I.

The next piece of hardware critical to the operation of the dual-slot heat pipe is the baffle. Ideally, both edges of the baffle should just touch the inner walls of the tube along its entire length. This divides the pipe into two separate regions, a liquid and a vapor channel, and completely encloses the grooves so they can operate as capillary passages to pump the liquid between the two channels. Unfortunately, it is impossible to machine both the width of the baffle and the inner diameter of the grooved tube to a zero tolerance for a perfect fit. The variations in width and diameter can either create a gap between the baffle and the wall or score the grooved walls at specific points along the length of the pipe during insertion of the baffle. Either condition will adversely affect the performance of the heat pipe. Three different baffle configurations were designed, built, and tested. A brief description of the advantages and disadvantages of each design follows.

Flat Baffle

The flat baffle assembly, shown in Fig. 3, consists of a 0.40-in. thick aluminum strip held down against the walls of the pipe by a spring that extends down the full length of the pipe. In theory, the thin baffle should be flexible enough to adjust to machining imperfections and maintain a constant baffle-wall interface. The major disadvantage of this design is in inserting the springs into long heat pipes. Pipes S/N 201, 203, and 301 were tested with this type of baffle configuration.

D-Baffle

The D-baffle (Fig. 4) is made by mechanically flattening one side of a small diameter tube and cutting short slots at the 6:00 o'clock position along the entire length of the baffle. It is more rigid than the flat baffle, so the one long spring needed to hold down the flat baffle can be replaced by many shorter lengths of springs evenly spaced along the length of the pipe. Therefore, insertion of this baffle is easier than insertion of the flat baffle. After completion of the thermal tests on pipe S/N 203, the flat baffle assembly was removed, replaced with a D-baffle assembly, and retested.

T-Baffle

Unlike both the flat and D-baffles, the T-baffle needs no springs to hold it in place (see Fig. 5). An aluminum T-shaped extrusion is chem-milled to the proper thickness, and the legs are machined to a size slightly smaller than the inside diameter of the tube. Inserting this baffle into any length of pipe is relatively easy, but the machining must be held to a very tight tolerance. Pipe S/N 210 uses this baffle design.

ASSEMBLY OF ALUMINUM HEAT PIPES

Before any heat pipe is assembled, all of its components are cleaned to Grumman standardized procedures. All aluminum hardware is cleaned with a non-etch alkaline cleaner, tap water rinsed; deoxidized with a chromated deoxidizer solution, tap water rinsed again, dried with filtered air, rinsed with anhydrous isopropyl alcohol, and finally dried with gaseous nitrogen heated to 160°F. All stainless steel hardware is acid cleaned, tap water rinsed, passivated, tap water rinsed, filter air dried, alcohol rinsed, and dried with heated nitrogen.

When assembling flat baffle and D-baffle test articles, the baffles are inserted in tubes and allowed to rest against the grooved walls. The springs are inserted

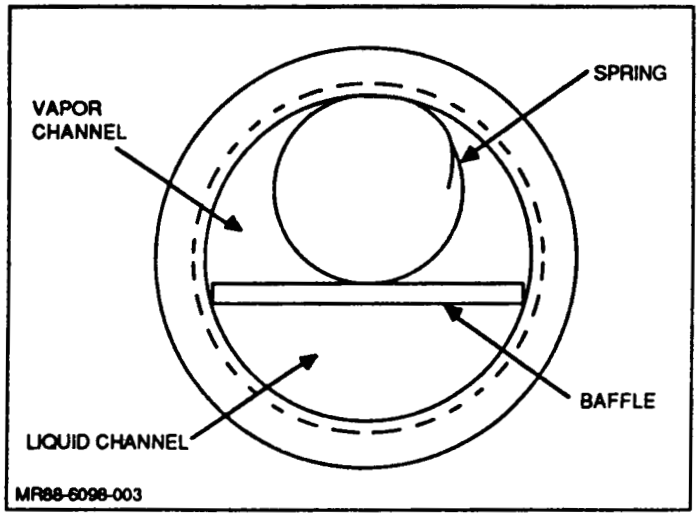

Figure 3 Flat Baffle

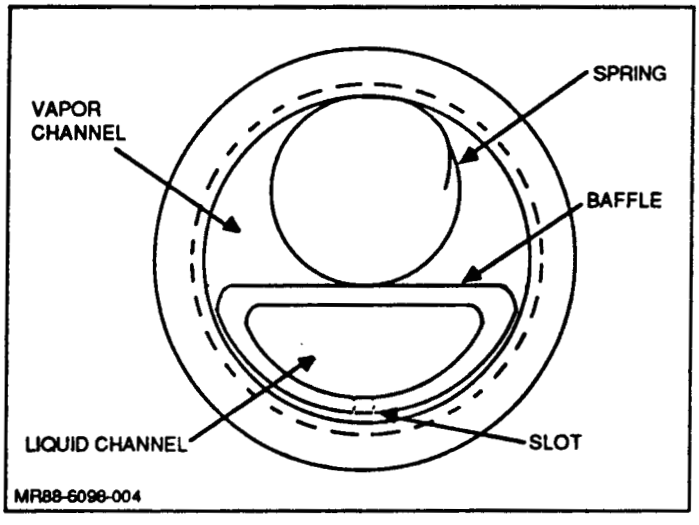

Figure 4 D-Baffle

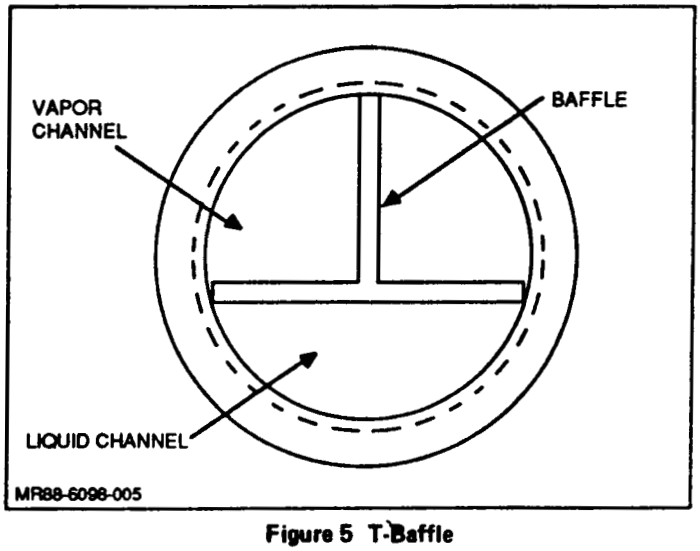

Figure 5 T-Baffle

into the vapor channel by stretching the spring apart, thus reducing its outside diameter so that it does not touch the walls of the tube. A small diameter stainless steel rod with a notch on its end is slid down the center of the spring and hooked on the end wire. By pulling on a piece of wire looped around the other end wire, the spring is stretched and readied for insertion. Once in place in the tube, the pressure on the spring is released, allowing it to return to its original shape pushing the baffle securely against the walls of the tube. The rod and wire are pulled out of the tube and used on another spring. The only drawbacks to this method of spring insertion is that the spring will damage the grooves at the 12:00 o'clock position when it is released.

When assembling T-baffle heat pipes, the baffles must be slightly smaller than the tube ID or the baffle will score the grooves along the entire length of the tube during its insertion. A sizing guide was made by drilling a hole in a 2 in. block of stainless steel. The aluminum baffle, being softer material than stainless steel, will deform slightly when slid through the sizing guide a few times, ensuring that the entire length of the baffle is a uniform width. The tube is kept straight by clamping it in the V of a heavy gauge angle iron. An aluminum rod bolted to one end of the T-baffle is used to pull the baffle through the tube. For the insertion, the baffle is positioned into the pipe upside down (i.e., the center leg of the T is at the 6:00 o'clock position) so that the grooves at the liquid-vapor channel interface are not damaged. During all ground testing, the pipe is orientated so that this center leg is at the 12:00 o'clock position and thus the vapor channel is above the liquid channel.

For heat pipes S/N 201 and 203, after baffle insertion, one end is arbitrarily picked as the evaporator end, and its liquid channel welded shut. The ends are sealed with Swagelok end cap fittings. Nickel felt metal is used to plug up the gap between the end of the baffle and the beginning of the end cap on the condenser end of the pipe. For pipes S/N 210 and 301, lift tests were done on all components before final assembly, so lift test extensions (described later in more detail) are welded in place. The lift test results are used to pick which components are to be used as the evaporator and condenser, then the final assembly of the heat pipes is completed.

Heat pipes S/N 201 and 203, being only 6 ft in length, could each be made from one length of tubing. However, pipes S/N 210 and 301, being 20 ft in length, were fabricated in sections that had to be coupled together. The two sections of S/N 210 were coupled together by welding an aluminum tube modified into a D-shape

that could fit in the liquid channel of each section. To connect the two vapor channels, an aluminum tube or sleeve with an 0.75-in. ID was slid over the outside of the heat pipe and welded in place over the gap between the two sections. The ends of the 20-ft heat pipe were sealed the same way as pipes S/N 201 and 203, except that the nickel felt plug at the condenser end of the pipe was not used. Instead, the liquid channel was welded shut, and small 0.040-in. vent holes were drilled in this weld.

The 18-ft transport/condenser leg of pipe S/N 301 was coupled together from two 9-ft sections using the same method as on pipe S/N 210. In this case, however, the transport end of the leg is welded to a manifold that in turn is connected to four 2-ft evaporator legs. The manifold consists of separate channels for the liquid and vapor flow drilled out of a solid block of aluminum. The liquid channel at the ends of the evaporator and transport/condenser leg inserted into the manifold are welded shut. Holes are drilled at the 12:00 and 6:00 o'clock positions so the vapor and liquid channels of the five different legs will match up with the vapor and liquid channels of the manifold when they are inserted. After the lift tests confirm that the four evaporator legs are communicating with the transport/condenser leg, all the legs are welded in place to the manifold. The condenser end of the pipe is sealed with a Swagelok end fitting with attached charge tube and valve. The ends of the four evaporators are welded shut because their non-circular shape prohibits the use of Swagelok fittings.

LIFT TEST PROCEDURES

The original test plan was to build two separate pipes for each design, one dedicated to lift tests and the other to thermal tests. Pipe S/N 202 was the lift test pipe for S/N 201 and 203. The prevalent thinking at the time was that if the fabrication and assembly techniques were the same for both heat pipes, then the effective gap width calculated for the lift test pipe would be applicable to the thermal test pipe. However, the variations in groove profiles noted previously and the variation in thermal performance between pipes S/N 201 and 203 (discussed later in this report) proved this idea to be wrong. For pipes S/N 210 and 301, lift tests were done on the same hardware later used for thermal testing.

All the pipes under test, whether lift or thermal tests, are placed on a rigid support beam so the pipe can be tilted without bending. Figure 6 shows pipe S/N 202 modified for list tests. The liquid channel is welded shut, and two tubes are welded in two holes at the 6:00 o'clock position. (The third tube at the 12:00

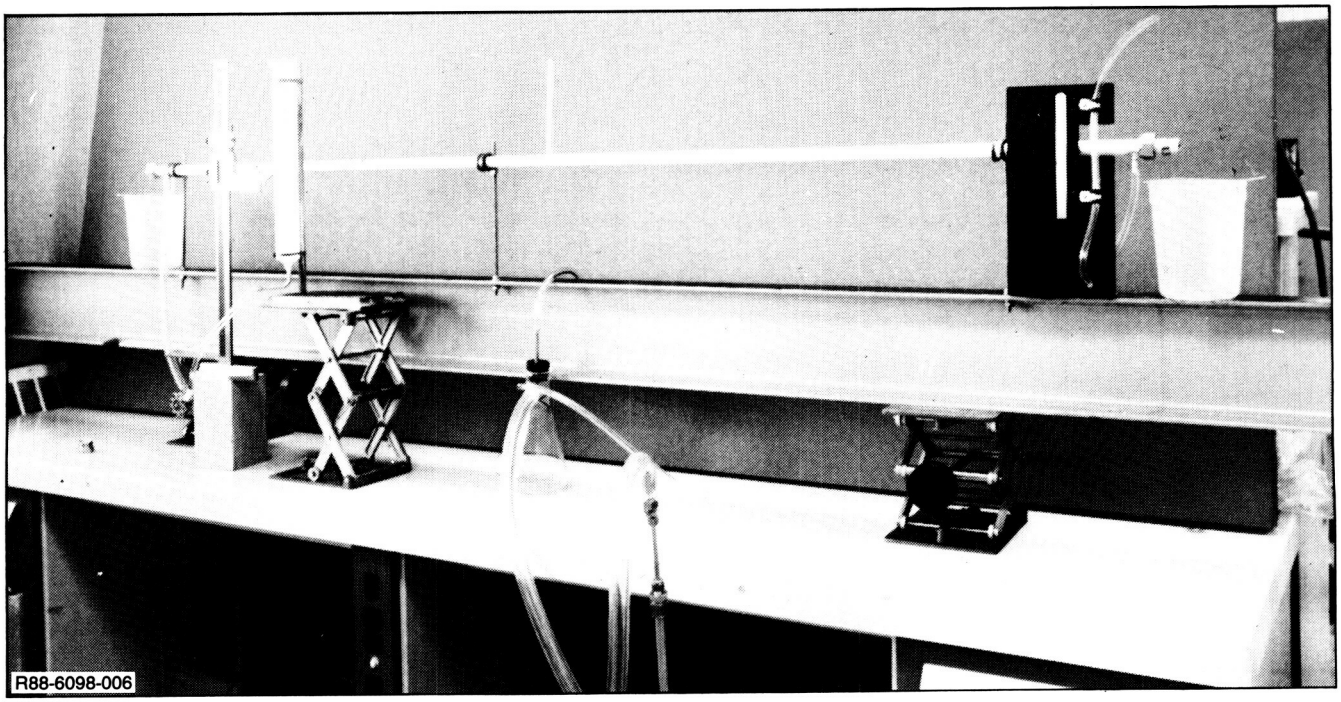

Figure 6 Lift Test Setup for Pipe 202

o'clock position, where a vacuum pump could be attached in case priming problems occurred, was not used.) A reservoir is attached to one of these vertical extensions with clear plastic tubing. A piece of plastic tubing forms a U-shaped manometer at the other end. The lift test setup for pipes S/N 210 and 301 differ in that an aluminum tube modified to fit in the liquid channel of each pipe is welded on each end, and a reservoir is attached to both of these horizontal extensions.

The procedure for all lift tests is the same. With the pipe level, the pipe is primed with a fluid, either acetone of isopropyl alcohol, by filling the reservoir until excess fluid drips out the ends of the pipe through the open vapor channel. The reservoir is lowered until the fluid level in the reservoir rises abruptly, indicating a break in the meniscus at the largest gap somewhere along the length of the pipe. The difference in the height of the reservoir is the amount of lift that can be maintained by this gap. To get an idea of where this gap is, we raise either end of the pipe slowly while the reservoir remains fixed. A break occurs when the liquid level in the reservoir(s) increases abruptly and an air bubble appears in the plastic tubing at the highest end of the pipe. If one end of a pipe cannot hold as much tilt as the other end, then that half of the pipe contains the large gap. The end of the pipe that can hold the most tilt is used as the evaporator of the heat pipe.

LIFT TEST RESULTS

Table II shows the results of all components lift tested. The amount of lift each component held is converted into an effective gap or slot width using the following equation:

$$\text{slot width} = \frac{2\sigma}{\rho g h} \qquad (1)$$

where σ = surface tension of fluid, ρ = density of fluid, and h = tilt. Conversely, the static wicking height for an ammonia charged pipe is also calculated from Equation 1 by rearranging the equation and solving for h using the fluid properties of ammonia.

The two sections of pipe S/N 210 (S/N 04-210 and 06-210) were lift tested individually, but the final assembled pipe was never lift tested.

The two 9-ft pipes used to form the transport/condenser leg in pipe S/N 301 each maintained a minimum of 1.8-in. tilt with isopropyl alcohol (0.0047-in. slot) individually, but when coupled together held only 0.97-in. tilt (0.0090-in. slot) at both ends of the pipe. This indicates the coupling method may have "lifted" the baffle assembly away from the grooved wall of the tube.

Evaporator leg S/N E3-301 had the worst lift of the five legs tested and so was not used in the final assembled heat pipe. During the lift testing of the final

TABLE II LIFT TEST RESULTS

S/N	Lift Test Fluid @ 293 K	Average Tilt (in.)	Static Wicking Effective Slot Width (in.)	Height with Ammonia @ 295 K (in.)
202	Acetone*	3.00	0.0030	3.62
04-210	Acetone*	2.23	0.0040	2.69
06-210	Acetone*	1.69	0.0053	2.04
12-301	Isopropyl alcohol	1.84	0.0047	2.27
13-301	Isopropyl alcohol	1.95	0.0045	2.40
301-Cond	Isopropyl alcohol	0.97	0.0090	1.20
E2-301	Isopropyl alcohol	2.40	0.0036	2.96
E3-301	Isopropyl alcohol	0.87	0.0100	1.07
E6-301	Isopropyl alcohol	2.13	0.0041	2.63
E7-301	Isopropyl alcohol	1.47	0.0059	1.81
E8-301	Isopropyl alcohol	1.46	0.0060	1.80
301**	Isopropyl alcohol	0.70	0.0125	0.86

* @ 300 K

** Lift test data were inconsistent – ranged from 0.5 to 1.0 in.

R88-6098-023

assembled version of pipe S/N 301, an air bubble never appeared at the end of any of the evaporator legs when the reservoir level increased abruptly. An explanation for this is that the break may have occurred in the condenser leg, and the air bubble was trapped in the manifold.

CHARGING THE HEAT PIPE

Each thermal test article was proof pressure tested with gaseous nitrogen to 500 psia (1.5 times the maximum operating pressure of the heat pipe). Next, the heat pipe was helium leak checked by drawing a vacuum with the detector on the inside of the pipe and spraying helium on all welds and fittings. Only a leak rate of 10^{-7} standard cc/s or less was accepted.

All the heat pipes underwent a Grumman standardized vacuum bakeout and charging procedure (Ref 4) to ensure that no contaminants or noncondensible gases (NCG) were present. However, if any pipe displayed abnormalities during its operation, we performed an NCG test, which consists of holding the pipe vertically, or as near vertical as possible, and establishing a large temperature differential between each end of the pipe. The end of the pipe with the valve must be at the top of this vertical orientation. Depending on what working fluid is in the pipe, one of the two methods described below is used.

For most fluids, the entire pipe is insulated except for a small area at the very top, which is left exposed to the ambient air. Next, a large amount of heat is applied to the bottom of the pipe. This method was not used with pipes containing ammonia because the internal vapor pressure at the elevated temperatures is larger than the pipe's proof pressure. However, it was used with heat pipes 201 and 203 having acetone as a working fluid. For ammonia pipes, the bottom of the pipe is left exposed to the ambient air and the top is cooled with liquid nitrogen (LN_2). With either method, if any NCG is present in the pipes, a low temperature "slug" will sit at the top of the pipe, where the internal pressure is at a minimum. This slug is at a lower temperature than the rest of the condenser since it is not transporting any heat. By quickly cracking the valve open one can remove the NCG or "burp" it from the pipe.

In our tests the pipes were filled with a slight amount of excess fluid to allow for uncertainties in the calculated amount required. This was necessary because small deviations in baffle dimensions can result in appreciable variations in the volume of the liquid channel. In addition, the volume of the liquid phase changes as the fluid temperature varies. The excess fluid typically ranged from 10-15% of the

full charge calculated from the heat pipe geometry. When a heat pipe is ground tested at a slight adverse tilt, the excess liquid accumulates at the end of the condenser. The puddle height must be taken into account when comparing test data with performance predictions.

THERMAL TEST OBJECTIVES

The primary objectives of the thermal testing program were to confirm the computer codes methodology and to evaluate the evaporation and condensation heat transfer film coefficients. Since the tests were conducted on the ground, we had to ascertain the effects of gravity in order to extrapolate the results to zero g. Therefore, the tilt of the heat pipes was varied and the maximum thermal transport capacity of the heat pipes determined for a range of tilts. Figure 7 shows a typical plot of predicted values of maximum thermal transport capacity as a function of tilt for various temperatures of the heat pipe working fluid. The dimensions of the heat pipe correspond to those of pipe S/N 210.

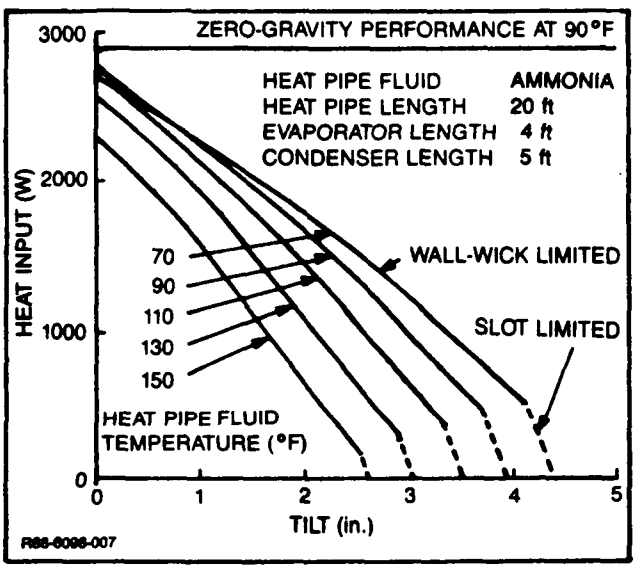

Fig. 7 Predicted Heat Pipe Performance for Ground Testing

THERMAL TEST SETUP

Once charged with a working fluid, the heat pipes were prepared for thermal testing. Preparations include application of a metallic (nichrome) ribbon to the evaporator section for electrical heat input and attachment of thermocouples at various locations along the length of the pipe. Thermal insulation is wrapped around the evaporator and transport sections of the heat pipes. Shower-head canisters are

placed on the condenser to provide cooling by tap water, which is sprayed over the full 360-deg circumference of the condenser. The condenser end of the heat pipe is placed over a trough to collect the drain water.

For the 6-ft-long heat pipes (201 and 203), the heater ribbon was applied in strips along the top quadrant of the outer diameter of the heat pipe evaporator sections. Thermocouples were placed at various axial locations along the heat pipes at the 12:00, 3:00 and 6:00 o'clock circumferential positions. Because of the limited area over which the electrical heating could be applied, the practical power limit of the heater ribbons was only 800 W, whereas the theoretical maximum thermal transport capacity of the 6-ft heat pipes (with ammonia) is approximately 3 kW at low values of tilt. This means that for ammonia, the limits of heat pipe can be approached only for large values of tilt. Therefore, tests on these heat pipes were also conducted using acetone as the working fluid. Because acetone is not as good a heat pipe fluid as ammonia, its performance limits were easier to reach, and the heat pipe could be tested up to performance limit over a wide range of tilts.

For the 20-ft heat pipe (210), some initial tests were performed with the heater ribbon applied in the same manner as the 6-ft heat pipes. For later runs, a 4-ft-long aluminum "saddle" was adhesively bonded to the top of the evaporator section using a silver filled epoxy with a high thermal conductivity. The heater ribbon was then applied to the flat surface on the top of the saddle. This provided more surface area for applying the heater ribbon and allowed greater heat input to the evaporator (up to approximately 2400 W). The saddle also resulted in a more even distribution of heat as well as a more realistic simulation of the intended heat input in the flight hardware. The saddle covered a 110-deg arc over the top of the heat pipe. Thermocouples were imbedded in it at the 12:00 and 1:00 o'clock positions via slits and drilled holes. The remaining thermocouples were placed at the 12:00, 3:00, and 6:00 o'clock positions at various locations along the length of the pipe.

For the multi-leg evaporator heat pipe (301), an integral saddle-like flange was built into each of the four evaporator legs. Thermocouples were pinned in at the 1:00 o'clock positions beneath the flange, and the 12:00, 3:00, and 6:00 o'clock positions elsewhere on the pipe.

Figure 8 illustrates the meaning of the phrase "adverse tilt" (vertical elevation of extreme end of evaporator above extreme end of condenser). When the evaporator end is beneath the condenser end, the pipe is in a "reflux tilt." Figure 9

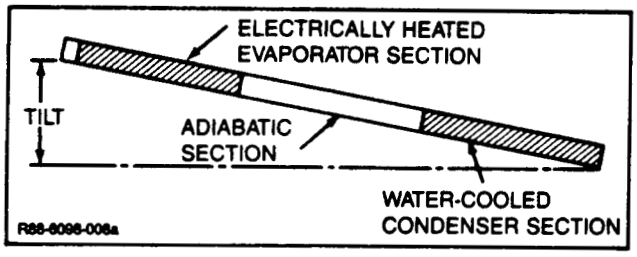

Figure 8 Heat Pipe Test Article Sections

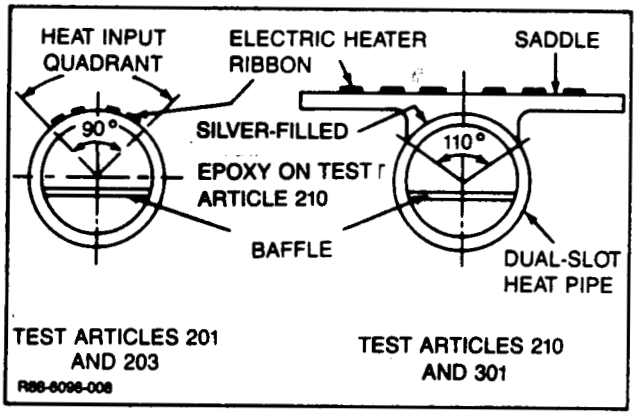

Figure 9 Evaporator Configurations for Aluminum Dual-Slot Heat Pipe Test Articles

shows the placement of the heater ribbon on the heat pipe circumference (for pipes 201 and 203) and on the flange (for pipes 210 and 301).

Figure 10 shows the two 6-ft heat pipes prior to application of heater ribbon and thermocouples. Figure 11 shows a 6-ft-long heat pipe mounted on its support beam with insulation around the evaporator and transport sections, and a water-cooling jacket around the condenser. Figure 12 shows the same heat pipe setup along with the 220-V Variac power supply used for varying heat input and a Fluke Model 2240B data logger used for recording thermocouple readings. The electrical power input is measured by a voltmeter and ammeter.

Figure 13 shows the 20-ft-long heat pipe mounted on its test stand, prior to being wrapped with insulation. There was no saddle and the heater ribbon was applied directly to it. Figure 14 shows the same heat pipe with the saddle that was subsequently bonded to the top of the evaporator section. The same power supply and data logger were used for the 20-ft heat pipe as for the 6-ft heat pipes. In addition, a Bristol strip chart recorder was occasionally used to measure temperature oscillations that occurred during the operation of this heat pipe.

Figure 15 shows the multi-leg evaporator heat pipe (S/N 301) attached to its support beam prior to application of heater ribbon and thermocouples. The heater ribbon was applied to the flanges built into each evaporator leg. The remaining test setup for this heat pipe was the same as S/N 210.

THERMAL TEST PROCEDURES

For each thermal test run of every pipe tested, the heat pipe was started by cooling the condenser section and providing heat to the evaporator at low values of heat input and tilt (often at a level or a slight reflux tilt to ensure the liquid

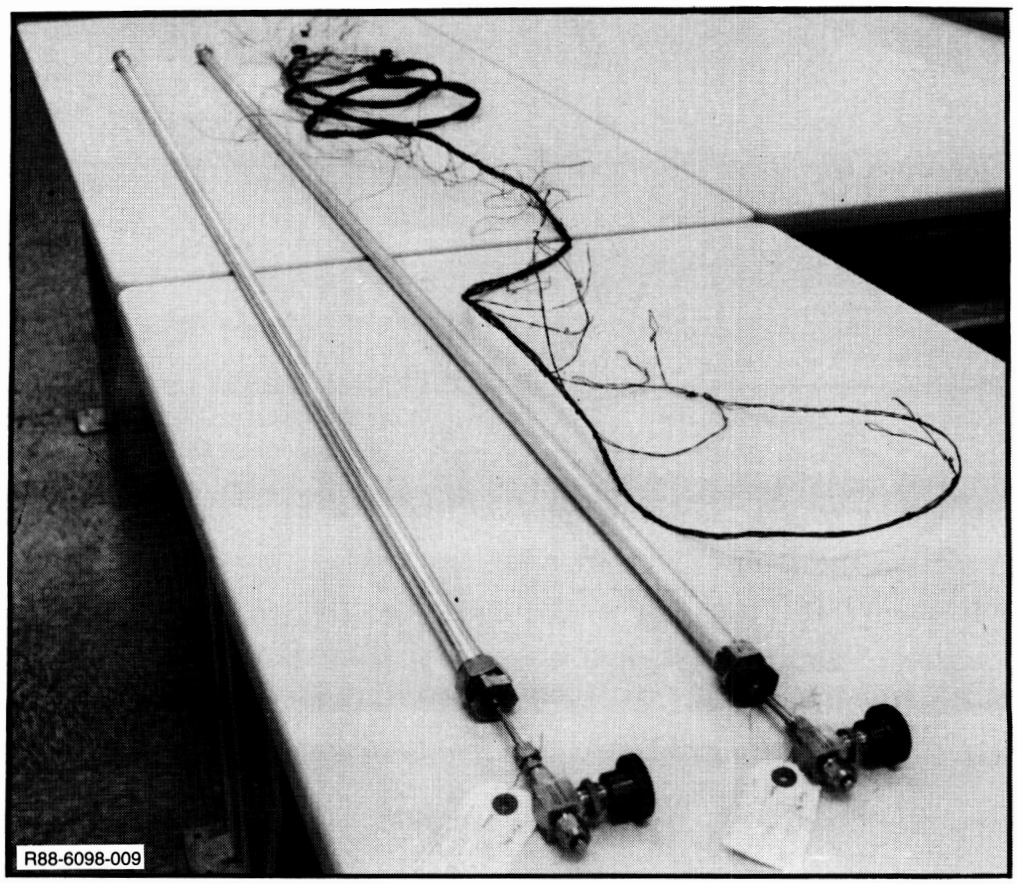

Figure 10 Aluminum Dual-Slot Heat Pipe Test Articles 201 and 203 (6-ft Long)

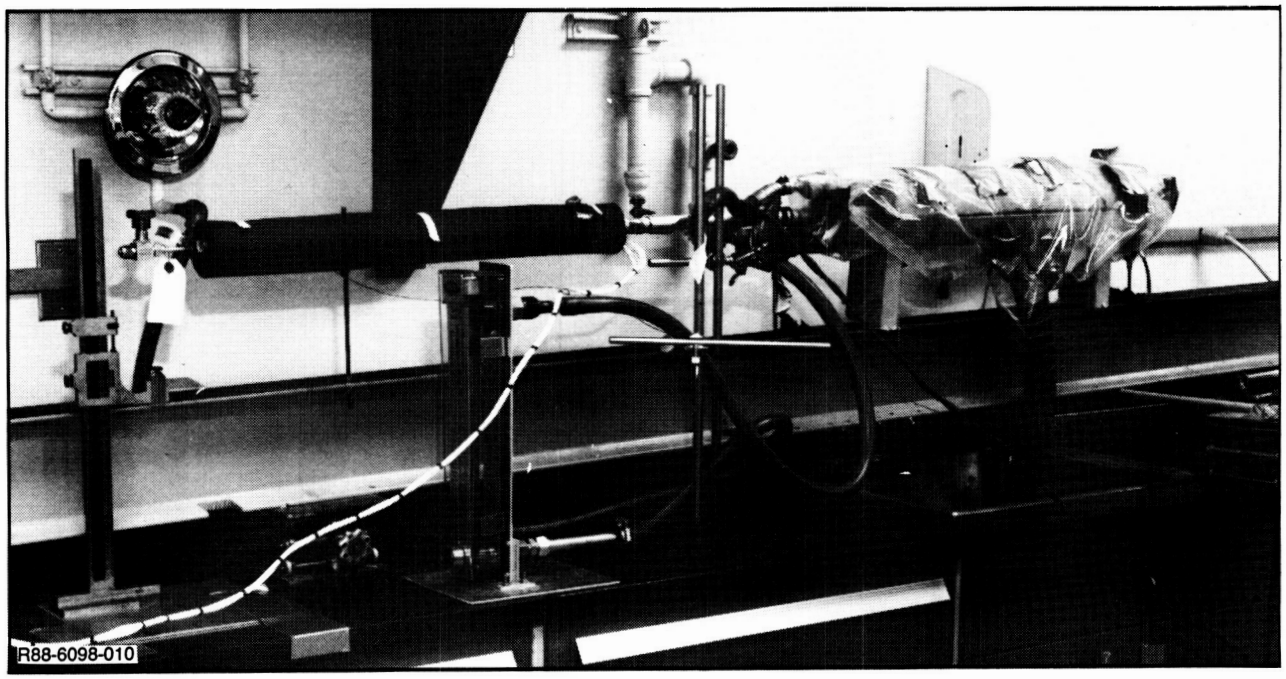

Figure 11 6-ft-Long Heat Pipe Mounted for Thermal Performance Testing

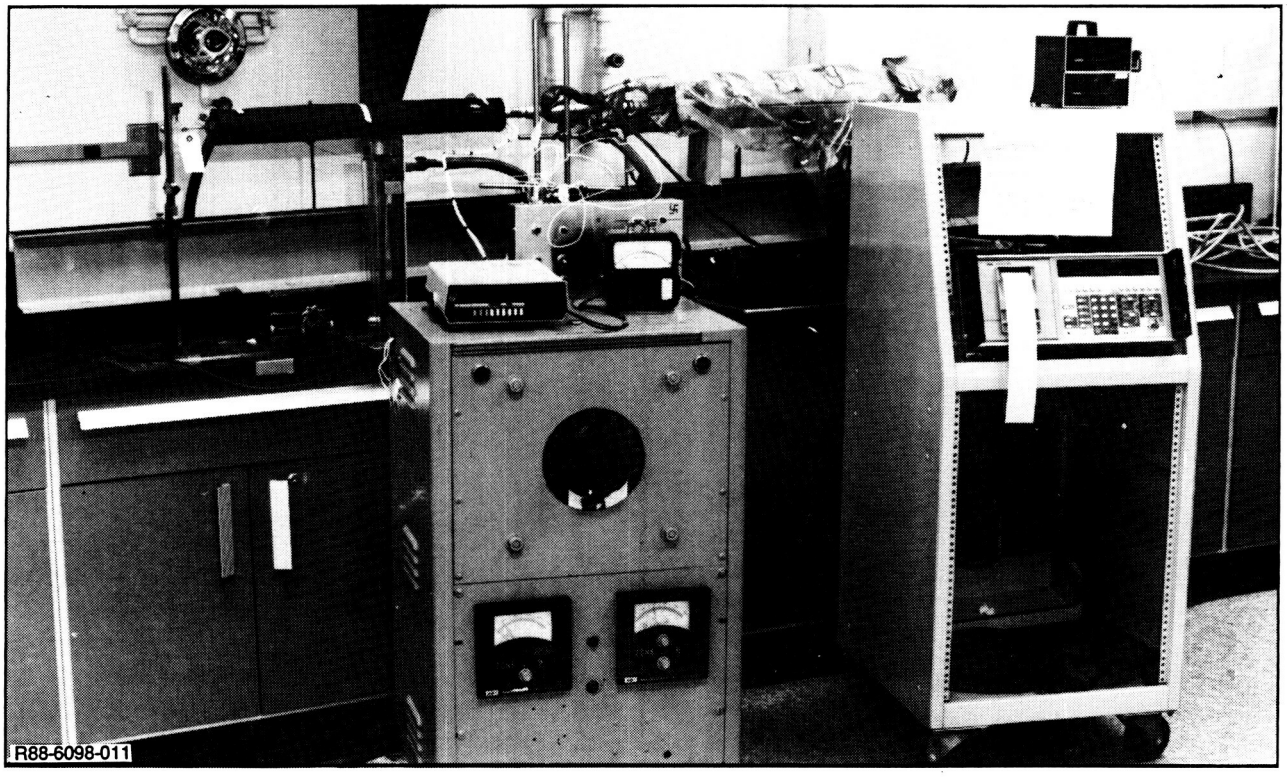

Figure 12 Apparatus for Heat Pipe Thermal Performance Testing

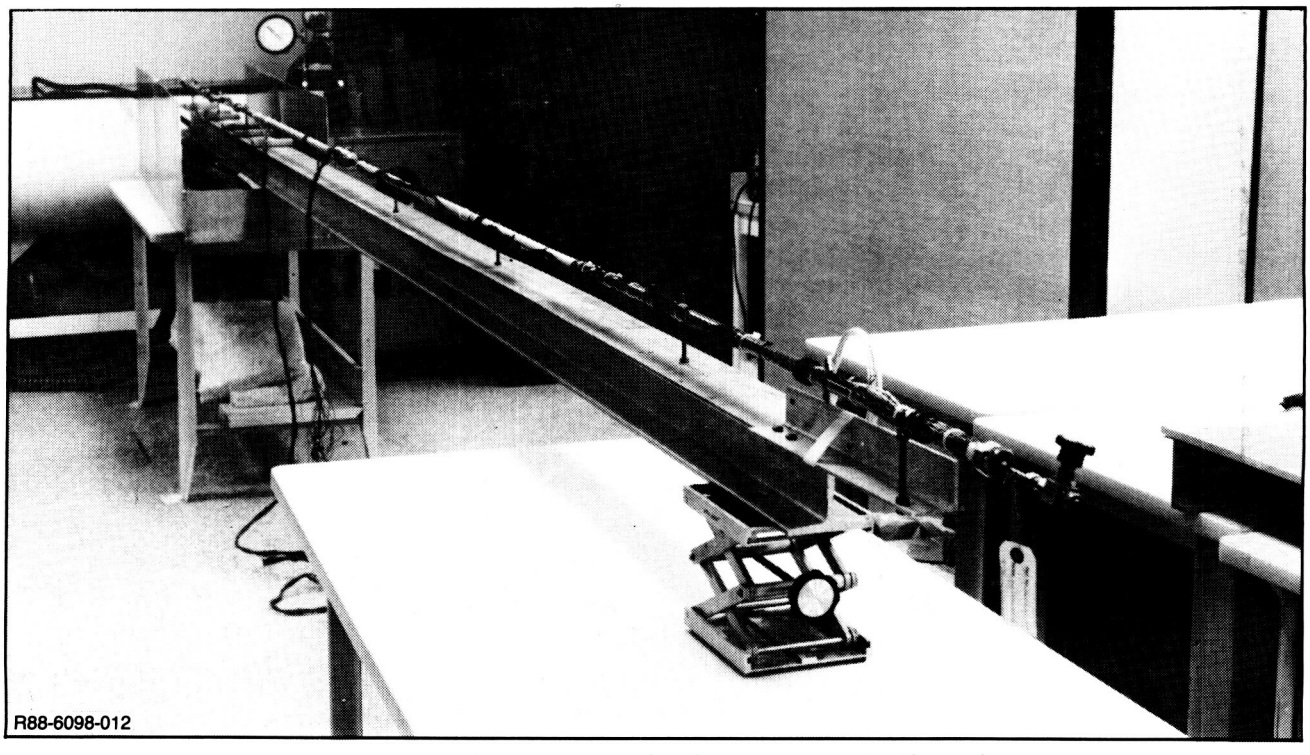

Figure 13 Aluminum Dual-Slot Heat Pipe Test Article 210 (20-ft Long)

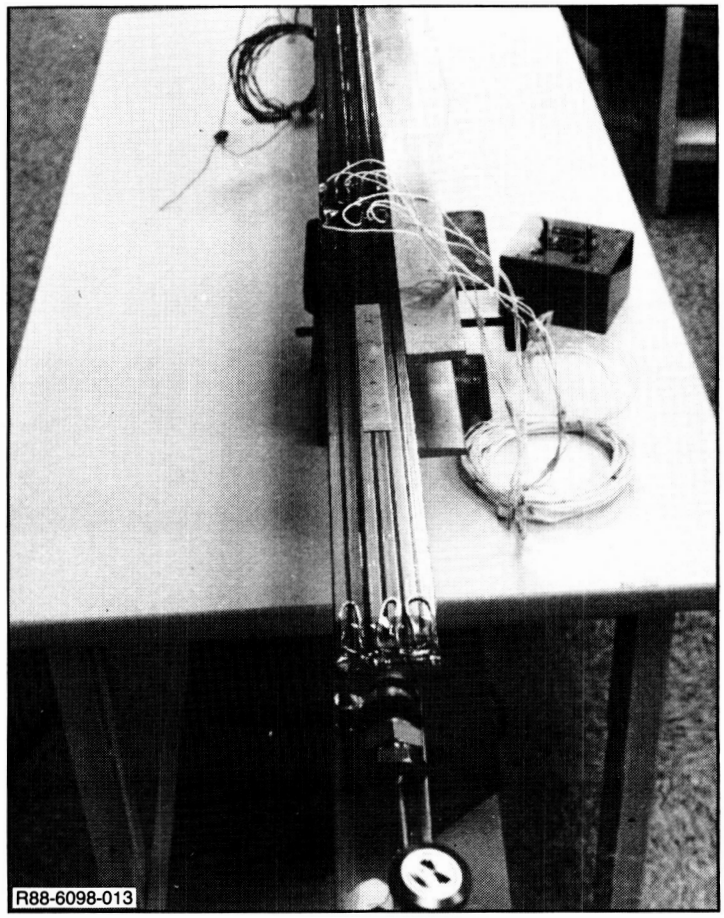

Figure 14 Evaporator Saddle for Heat Pipe Test Article 210

Figure 15 Multi-Leg Evaporator Dual-Slot Heat Pipe Test Article 301

channel was primed). Then one of two procedures was followed. Either the heat input was slowly raised to a specified value and the tilt increased in small increments, or the tilt is slowly raised to a specified value and the heat input incremented. Thermocouple readings were recorded periodically with the data logger at each test point. For heat pipe 210, several thermocouples were monitored continuously with a strip-chart recorder to indicate transients. After three cycles -- the amount of time needed to evaporate mass of charge three times at the preset heat input level -- the tilt or heat input was incremented to the next test point.

For each test run, a limiting value of tilt or heat input was reached beyond which the temperatures in the evaporator section would rise very rapidly, and the heat source had to be immediately removed to avoid overheating. The onset of such a condition was signaled by a rapid rise in the temperature of a continuously monitored thermocouple located at the end of the evaporator section.

This is noted as an "unstable" condition since the temperature would continue to rise if the heat input continued. The unstable condition arises from an imbalance between the rate of heat input and the rate of heat absorption by means of evaporation of the fluid in the grooves. This imbalance is associated with dryout of the evaporator grooves when the wicking capability of the grooves is exceeded, or loss of capillary integrity when the slot meniscus can no longer support the pressure differential between the vapor and liquid channels.

THERMAL TEST RESULTS

The heat pipe operation was found to be very sensitive to test conditions and startup procedures. A large number of test runs aborted due to premature dryout, depriming, or unsteady behavior. The remaining runs can be classified as "successful" relative to the abortive runs. Results from the "unsuccessful" runs are not reported here since difficulties experienced in starting the heat pipe resulted in no meaningful data.

Summaries of the test results and performance predictions for the three heat pipe test articles are shown in Figs. 16 through 19 as plots of heat input as a function of tilt. The test data are shown as short horizontal bars (at constant heat input) that extend from the highest tilt at which steady performance was achieved (open data point) to the value of tilt at which performance became unstable (solid data point). The performance limits predicted by the analytical models are shown in these figures as continuous solid or dashed lines.

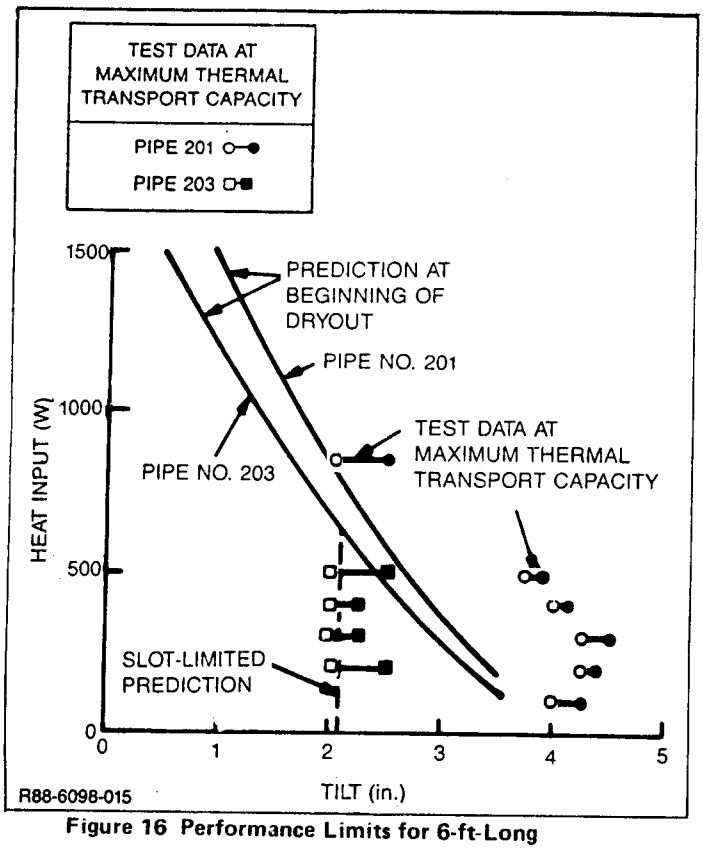

Figure 16 Performance Limits for 6-ft-Long Aluminum Test Articles Using Ammonia

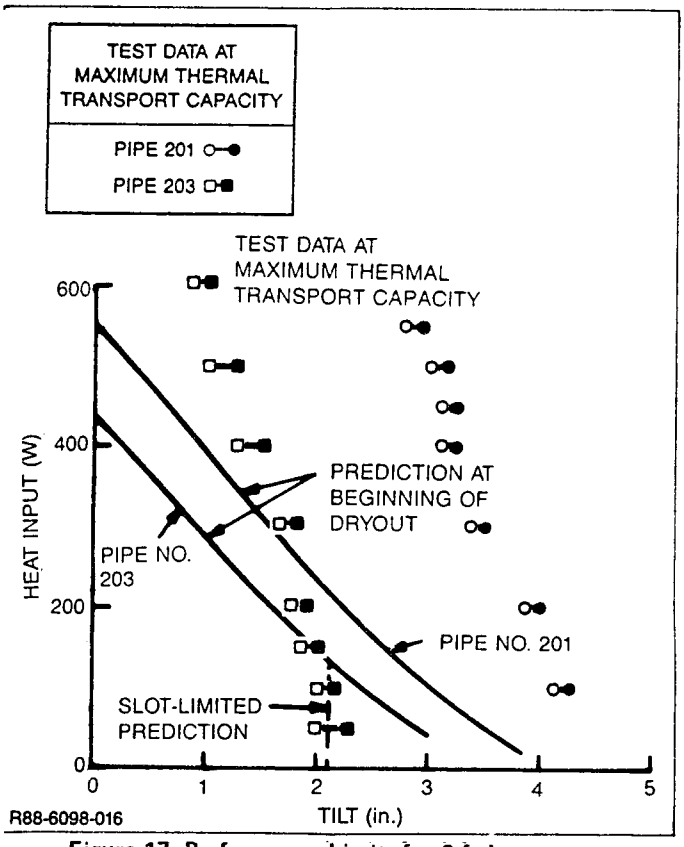

Figure 17 Performance Limits for 6-ft-Long Aluminum Test Articles Using Acetone

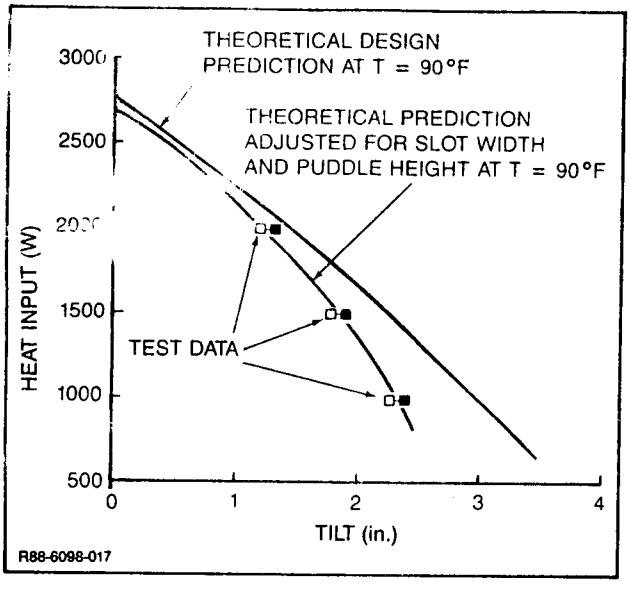

Figure 18 Performance Limits for 20-ft-Long Aluminum Test Article (No. 210) Using Ammonia

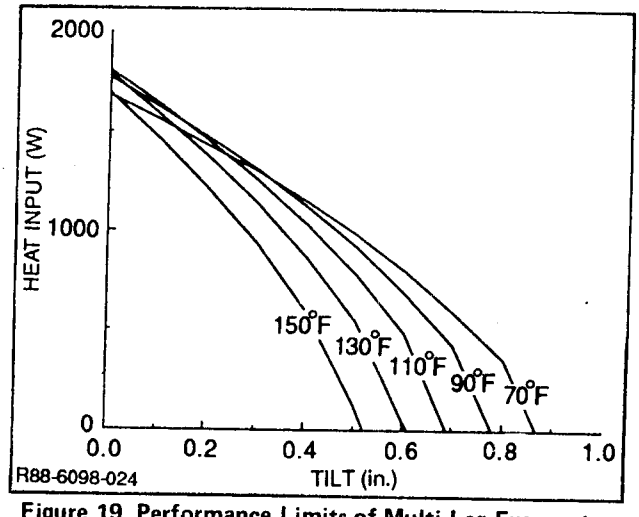

Figure 19 Performance Limits of Multi-Leg Evaporator Test Article (No. 301) Using Ammonia

Figures 20 through 22 show test data as plots of temperature differential between the wall of the evaporator section and the heat pipe working fluid as a function of heat input rate for constant values of tilt. The temperature of the wall of the evaporator is taken as the reading of a representative thermocouple on the top of the evaporator. The temperature of the working fluid is taken as the reading of a representative thermocouple on the adiabatic section of the heat pipe.

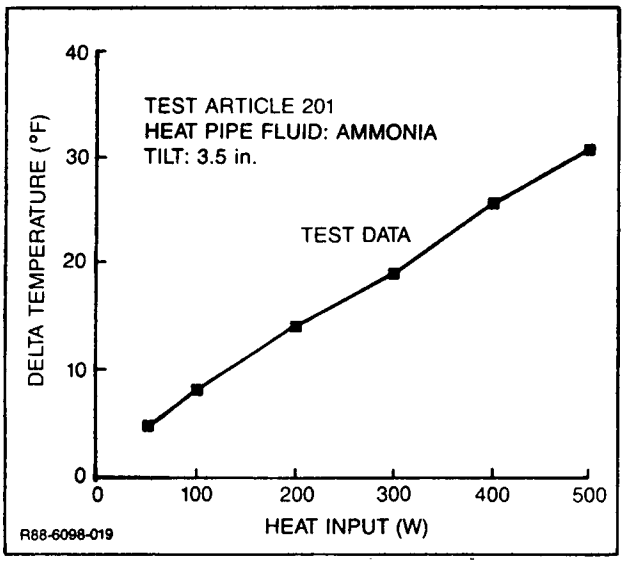

Figure 20 6-ft Heat Pipe (No. 201) Evaporator Temperature Differential with Ammonia

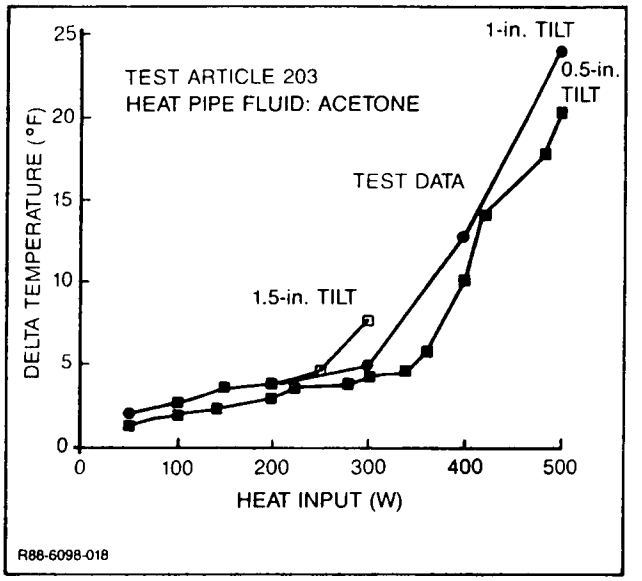

Figure 21 6-ft Heat Pipe (No. 203) Evaporator Temperature Differential with Acetone

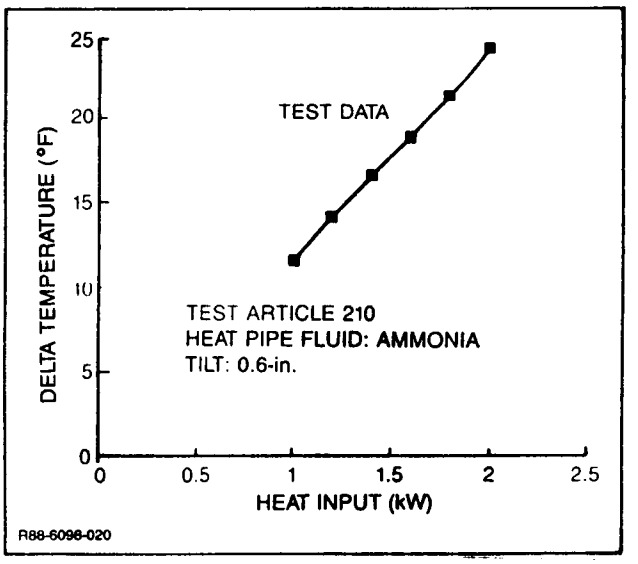

Figure 22 20-ft Heat Pipe (No. 210) Evaporator Temperature Differential with Ammonia

S/N 201 and 203

The two prediction curves shown in Fig. 16 for the 6-ft-long heat pipes with ammonia reflect the differences in groove dimension between test articles 201 and 203. These curves also show the effects of a puddle of excess liquid. In the case of pipe 201, the prediction corresponds to wall-wick limited performance. For pipe 203, the solid line corresponds to wall-wick limited performance, while the dashed line corresponds to slot-limited performance (based on an estimated slot width that best conforms to the test data).

As noted previously, the range of the data obtainable for the 6-ft-long heat pipes with ammonia is restricted, by heater ribbon limitations, to a low wattage compared to the expected capability with ammonia. Therefore, the range of heat input over which the data were obtained is too restricted to draw definite conclusions. The primary observations to be made from the test data shown in Fig. 16 are that (1) the performance limits attained for 201 during testing are generally higher than the predicted performance limits; (2) the differences between the test results for pipes 201 and 203 are greater than the predicted differences; and (3) the test data for pipe 203 follow the slot-limited performance prediction.

The apparent discrepancy between the test results and predictions for 201 may be attributed to an overly conservative analytical model of the grooves or to the effects of partial dryout beyond the point at which the analysis predicts onset of dryout. Although there is no evidence of partial dryout from Fig. 20 (which shows a line of virtually constant slope), this type of behavior is exhibited quite clearly in the tests with acetone (as will be subsequently described in conjunction with Figs. 17 and 21).

The significant difference in performance between heat pipes 201 and 203 can be attributed to differences in slot width between the two heat pipes. Although not confirmed by direct measurement of the slot widths, this conclusion is supported by test data that indicate virtually the same tilt limit for all values of heat input. This trend is characteristic of slot-limited performance.

The two prediction curves shown in Fig. 17 for the 6-ft-long heat pipes with acetone also reflect the differences in groove dimensions between test articles and the effects of a puddle of excess liquid. Wall-wick limited performance is shown by solid lines and slot-limited performance by dashed lines. Since acetone is a poorer heat pipe fluid than ammonia, a wider range of tilt limit values are evident for a comparable range of heat input. Some of the same conclusions can be drawn for heat pipes 201 and 203 from the data for acetone as for ammonia. Figure 17 shows

that heat pipe 201 has much greater tilt capacity than 203, and the test data limits are generally higher than the predicted performance limits. However, insight into the apparent discrepancy between test results and predictions may be obtained by examining Fig. 21, where the slope of the line of temperature differential versus heat input takes a sharp upturn at certain values of heat input, depending on the tilt of the heat pipe. This indicates that the heat pipe functions with no dryout of the grooves for low values of heat input but exhibits partial dryout at higher values.

Thus, at least in the case of heat pipe 203 using acetone, there is evidence of operation in a partially dried out state. The heat input at which the heat pipe goes unstable is appreciably higher than that at which dryout begins. This may explain why the test results seem to be better than predicted. The predictions indicate the onset of dryout, whereas the heat pipe continues to function in a partially dried out state at higher heat input rates and tilts. However, the heat transfer efficiency of the heat pipe is lower in a partially dried out condition, as indicated by the steeper slope in this region of Fig. 21. The points at which the sudden increase in the slopes of the lines occurs correspond reasonably well with the points at which dryout is predicted to begin, thus supporting this conclusion.

S/N 203-D

After completing thermal tests of S/N 203, we disassembled and reassembled the pipe with a new baffle configuration, the D-baffle. This modified version of the heat pipe is called S/N 203-D. No lift tests were done on this pipe and only limited thermal tests were completed since we did not wish to impact the scheduling of tests on S/N 210, which was being fabricated at the time.

From the start of testing, S/N 203-D experienced startup problems and no successful test runs were ever completed. The temperatures in the evaporator section would oscillate or cycle by 20°F or more and burn out at tilt and heat inputs far below the values maintained by S/N 203 with the flat baffle. This poor thermal transport performance could have been caused by a poor assembly technique rather than a flaw in the D-baffle design.

The peculiar temperature oscillations while the pipe was operating at steady-state are thought to be caused by vapor trapped in the liquid channel and unsettling the flow to the wall grooves. Vent holes were drilled in the condenser end of the baffle so that at reflux tilt the vapor could escape; however, the temperature oscillation continued. We hypothesize that the vapor may be created by

boiling in the liquid channel. The lowest pressure in the pipe exists in the liquid channel at the evaporator end of the pipe. Saturated liquid from the condenser heated by the hot vapor as it moves from the condenser to the evaporator may become superheated enough to cause boiling at this low pressure point of the pipe. As the vapor builds up, the liquid flow through the slots to the wall grooves is interrupted and local dryout occurs. When the vapor vents through the slots, the liquid feed to the wall grooves returns and the temperature drops. Then the cycle starts over again.

S/N 210

A few successful test runs were obtained in the early stages of testing this heat pipe. The test data from these successful runs are shown in Fig. 18. The upper curve indicates the theoretical performance under ideal design conditions of zero slot width (no gap between baffle and pipe wall) and no excess charge. The lower curve indicates the predicted performance when adjusted to account for the actual slot width (estimated from lift test results) and the puddle due to the charge quantity margin. The temperature of the adiabatic section of the heat pipe ranged from 79°F to 101°F for the three test points shown. The predicted performance shown in the figure was calculated at 90°F. The test data are extremely close to the adjusted performance predictions.

The temperature differential plotted in Fig. 22 is the difference between the temperature of the evaporator (as measured by thermocouples imbedded in the saddle) and the temperature of the adiabatic section (as measured by thermocouples attached to the heat pipe in the adiabatic section). The data fall along a relatively straight line, indicating that the circumference grooves provide adequate wall wicking right up to the point of unstable operation. The calculated values of heat transfer film coefficient ranged from approximately 1200 to 1500 Btu/hr-ft^2°F. These values are in the expected range. The calculations are based on the surface area inside a smooth wall with an area of 110 deg, corresponding to the region of contact between the heat pipe and the saddle.

The performance of the 20-ft heat pipe (S/N 210) had been erratic from the start of testing. Large amplitude temperature oscillations of as much as 70°F were noted at specific thermocouples in the evaporator section. Because the temperature oscillations appear to be similar to those observed in S/N 203-D, trapped vapor or boiling is assumed to be the cause of the startup problems. A static priming test

was conducted with an ultrasonic sensor to determine if vapor was present in the liquid channel before power was applied to the pipe. To calibrate the sensor, a short sample of the heat pipe assembly previously removed was modified for use as the reference standard. The tilt of the pipe was adjusted until the sensor--placed at the 6:00 o'clock position on the evaporator section of the pipe--indicated that the liquid channel was full. Then the pipe was checked with the sensor at various points along its length to be sure the liquid channel was primed everywhere before applying any power. Even though the ultrasonic sensor signaled the pipe was full on three separate test runs, the pipe went unstable shortly after nominal power was applied, indicating the startup problems were caused by boiling..

Because the performance of the pipe degenerated with time and handling, we hypothesize that damaged grooves are another cause of the erratic performance. Large deflections in the pipe can occur during handling given the pipe's long length, thin wall thickness, and the structural strength of aluminum. If the pipe does deflect, the baffle (being independent of the pipe) can deflect differently than the pipe, thus rubbing or "scouring" the inside walls of the pipe and damaging the grooves. To minimize deflection, the assembled pipe was mounted and leveled on a 4 x 4 x 0.3125-in. I-beam, which deflects only 0.12 in. in the middle if picked up at both ends. However, the pipe had undergone several "bake-out" and "charging" procedures because of modifications made to it, and, on one occasion, the pipe had to be removed from the I-beam to be cleaned. Even though extreme care was used when handling the pipe, it is possible the grooves were damaged.

A 3-ft section of the evaporator was removed from the pipe, dissected, and examined. Figure 23 presents photomicrographs of the tube section magnified 2 and 24 times, showing that the baffle assembly did score the grooves in the wall of the pipe. To what extent the grooves were damaged is difficult to ascertain. Examining a cross-section sample of the grooves is impractical since the damaged grooves lie along a very thin score line. Although there probably exists a method of measuring depth along one's line of sight, lack of time and funds prevented us from investigating it. However, visual inspection of the dissected section under a microscope does reveal that the grooves are not totally destroyed. Although the baffle does cut into the depth of the grooves, it does not cut all the way to the bare metal. It appears that liquid should have been able to wick past the score line and feed the wall grooves.

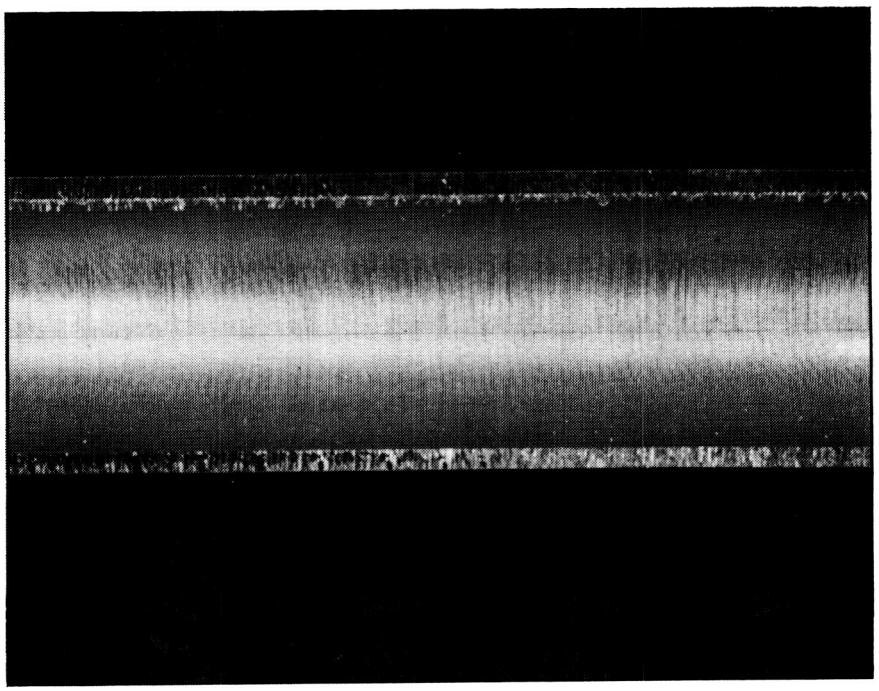

a. Magnification 2x

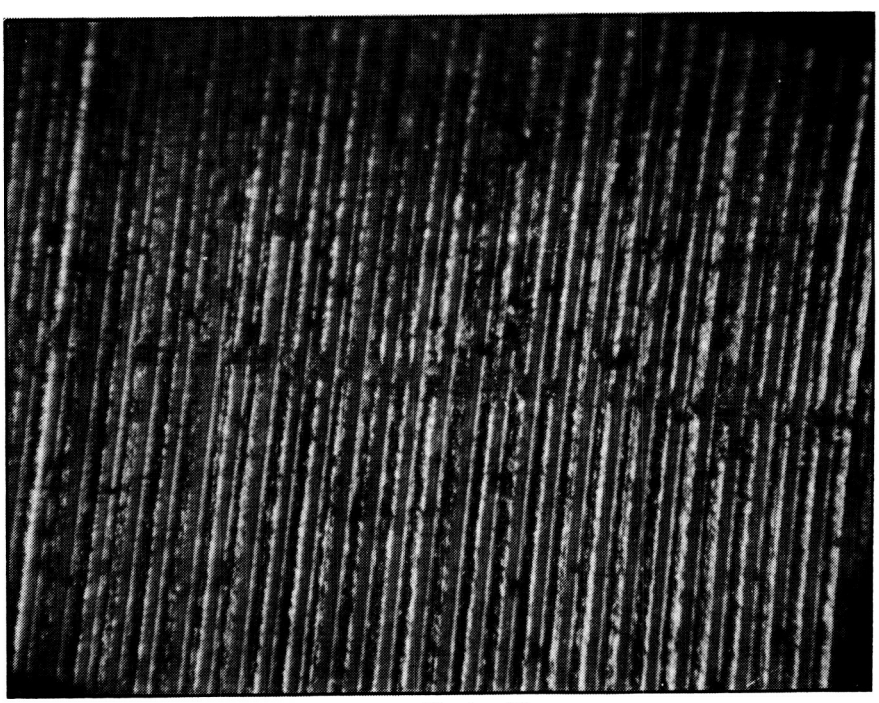

b. Magnification 24x

Figure 23 S/N 210 Groove Damage

S/N 301

Figure 19 is a graph of the predicted thermal performance of the multi-leg evaporator heat pipe (S/N 301) at various temperatures. All five curves reflect slot-limited performance due to the large effective slot width calculated from lift test results (0.0125 in.). No actual test data are shown on this graph because startup problems prevented any successful test runs. After applying power to the pipe, the temperature of the evaporator and transport section would steadily increase to the maximum safe operating temperature (130°F) before three evaporation cycles had passed. No matter what the level of heat input, the temperatures steadily increased without ever reaching a steady-state value. The condenser temperature profile was equal to the cooling water temperature (55-70°F). Transport-condenser temperature differences of as much as 50°F were present, indicating that the condenser was either flooded with excess liquid or blocked with NCG.

NCG tests proved no NCG was present, so liquid flooding was assumed to be the cause of the problem. However, the amount of excess charge (15%) was not enough to totally block the 5-ft condenser. The pipe behaved as if the liquid channel was slowly starving the evaporator over time, so we hypothesized that the baffle may have cut into the wall grooves as with S/N 210.

The pressure differential between the vapor and liquid channel is small at the condenser end so a reduction in flow area between the two channels could produce the flooding effect and slowly starve the evaporator which is 8 ft in total length as compared to the 5-ft condenser area.

A 3-ft section was cut from the end of the condenser, dissected, and viewed with a microscope. The groove profile was very similar to the one found in S/N 210 and shown in Figure 22. We were unable to measure the depth of the score in the wall grooves but, based on our visual findings, we recommend replacing the existing condenser with a new condenser leg that has a different baffle configuration and retest this heat pipe. Unfortunately, lack of funding and a tight schedule prevented the completion of this task.

FABRICATION OF STAINLESS STEEL HEAT PIPES

The first attempts at cutting grooves in stainless steel pipes using the same tooling and procedures as in grooving aluminum heat pipes produced limited results. The longest length of tubing that could be grooved before the single point cutters failed was 18 in. To ascertain if single point cutting was at all capable of cutting grooves in longer lengths of stainless steel, a tool life test was initiated. Different

cutter designs and cutting speeds were tested by cutting grooves on the outside diameter of a stainless steel bar. This allowed easy evaluation of the groove profile by putting the bar on a thread comparator. Also, by removing the cut threads, the same bar could be reused again and again. A copy of the test plan can be found in the Appendix.

Table III shows the results of the tool life test. The optimum tool design was found to be a C-2 micrograin with a 4-deg positive top angle and a 1.25 to 1.50-deg positive front angle coated with titanium nitride. This design cut a little over 30-in. of threads on a 2-in. diameter bar, which is equivalent to machining almost 8 ft of 3/4-in. OD tubing.

TABLE III TOOL LIFE TEST RESULTS

Tool Material	Coating	Tool Geometry		Equivalent Cut Length (in.)	Average Groove Depth (in.)
		Top (deg)	Front (deg)		
C-6 Micrograin	None	+4	+3	Tool failure	N/A
	None	−4	+1.25 to 1.50	Tool failure	N/A
	None	+4	+1.25 to 1.50	Tool failure	N/A
C-2 Micrograin	None	+4	+3	47.5	0.0033
	None	−4	+1.25 to 1.50	47.5	0.0033
	None	+4	+1.25 to 1.50	47.5	0.0048
	Ovonic	+4	+1.25 to 1.50	Tool failure	N/A
	Titanium nitride	+4	+1.25 to 1.50	95.0	0.0059

Optimum surface cutting speed = 80 SFM;
Groove pitch = 108 TPI

R88-6098-025

Unfortunately, we had limited success when this optimum cutter design was used to cut grooves inside the tubing. Because the ID of the stainless steel tubes was slightly larger than the ID of standard aluminum tubing, we could not use the same reaming tool to true up the tube. Due to budget and time constraints, we did not fabricate a new reamer. This proved to be a mistake, for the threads were lopsided in every length of tubing. On one side of the wall there were perfectly shaped grooves 0.006 in. in depth, but on the opposite wall the cutter barely scratched the metal. None of the cutters failed during machining the 10-ft lengths, but since the threads were lopsided, the effective length of the cut is obviously less than 10 ft.

CONCLUSION/RECOMMENDATIONS

The advantage of the dual-slot heat pipe design is that it can be assembled from materials other than aluminum, therefore it has the potential of being used in high temperature applications. Although it was shown in Task 1 of this contract to be a good candidate for the Space Station solar dynamic power module's radiator system, the problems encountered during thermal testing of hardware in Task 2 indicates that this heat pipe design is not mature enough to fly on the Space Station. The startup problems encountered with test articles 203-D, 210, and 301 should first be solved before testing heat pipes fabricated from other materials. The baffle configuration seems to be the critical component in whether or not the dual-slot heat pipe performs to predictions. Our hypothesis of the cause of the startup problems with S/N 301 is groove damage in the condenser section, which blocks the flow of condensate from returning to the liquid channel. We recommend fabricating a new condenser leg for heat pipe S/N 301 using a different baffle assembly configuration. Either one of the two baffle configurations described below can be used.

Aluminum Flat Baffle with Vent Holes

This is essentially the same design as presently used on pipe 301 but with vent holes drilled through the baffle plate. Since there is only a small pressure drop between the vapor and liquid channels at the end of the condenser, the vent holes can be much larger than the slot width. However, the size of the vent holes will fix the amount of reflux tilt that the pipe can hold.

The advantages of this baffle design are that (1) any liquid that collects on top of the baffle plate can get through to the liquid channel; (2) if the baffle damages the grooves and thus decreases the effective flow area between the vapor and liquid channel, the vent holes offer another path for liquid flow; and (3) any vapor trapped in the liquid channel can be vented by priming the pipe in a reflux position.

The disadvantages of this baffle configuration are that (1) it does not eliminate liquid hangup in fillets at the top of the vapor channel where the spring touches the top of the pipe; (2) there is limited space available on the end of the baffle to drill vent holes.

Stainless Steel Flat Baffle with Wire Screen or Felt Metal

With a stainless steel flat baffle, wire mesh screen or felt metal can be tack-welded around the baffle. The baffle is still held in place by springs so the

insertion method does not change. The advantages of this design are that: (1) screen or felt metal presents liquid with another pathway for it to go from the vapor to the liquid channel; (2) screening or felt metal may protect grooves from being damaged by the baffle. The only disadvantage is that more labor is required to tack-weld the screen or felt to the baffle.

The problems with both S/N 203-D and 210 are thought to be caused by trapped vapor or possibly boiling in the liquid channel. The same two baffle configurations discussed for the new condenser leg on S/N 301 can also be used in the evaporator of these two heat pipes. However, the baffle with vent holes is not recommended. The baffle in the evaporator must maintain a large pressure differential; thus, the holes would have to be very small, making them inefficient vent holes.

Since the screen-covered flat baffle may solve both evaporator and condenser startup problems with the dual-slot heat pipe, we recommend that the new condenser leg for S/N 301 be assembled with this type baffle. If this design proves to solve S/N 301's problem then the next heat pipe fabricated and tested could be a stainless steel/methanol article using this screen-covered flat baffle assembly.

To fabricate grooved stainless steel tubing we recommend reaming an annealed stainless steel tube true before cutting grooves with the titanium nitride coated cutter.

REFERENCES

1. Gustafson, E. and Carlson, A., Solar Dynamic Heat Rejection Technology, Task 1 Final Report, System Concept Development, NASA Contractor Report 179618, June, 1987.
2. Alario, J., Haslett, R., and Kosson, R., "The Monogroove High Performance Heat Pipe," AIAA Paper 81-1156, Presented at the AIAA 16th Thermophysics Conference, Palo Alto, California, June 23-25, 1981.
3. Alario, J., Brown, R. and Kosson, R., "Monogroove heat Pipe Development for the Space Constructible Radiator System," AIAA Paper 83, 1431, Presented at the AIAA 18th Thermophysics Conference, Montreal, Canada, June 1-3, 1983.
4. "Heat Pipe Manufacturing Study," Final Report prepared by Grumman for Contract NAS5-2316, August 1974.

BIBLIOGRAPHY

Carlson, A., Gustafson, E. and Roukis, S., "High Thermal Capacity Heat Pipes for Space Radiators," SAE Paper 871509, presented at the 17th Intersociety Conference on Environmental Systems, Seattle, Washington, July 13-15, 1987.

Carlson, A., Gustafson, E. and McLallin, K., "Solar Dynamic Space Power System Heat Rejection," presented at the 21st Intersociety Energy Conversion Engineering Conference, San Diego, California, August 25-29, 1986.

Carlson, A., Gustafson, E. and Ercegovic, B., "Heat Pipe Radiator Technology for Space Power Systems," AIAA Paper 86-1300, presented at the AIAA/ASME 4th joint Thermophysics and Heat Transfer Conference, Boston, Massachusetts, June 2-4, 1986.

Gustafson, E. and Carlson, A., "Heat Pipe Radiators for Solar Dynamic Space Power System heat Rejection," presented at the 22nd Intersociety Energy Conversion Engineering Conference, Philadelphia, Pennsylvania, August 10-14, 1987.

APPENDIX

TEST PLAN FOR THE SINGLE POINT CUTTING TOOL LIFE TEST

TEST OBJECTIVE

The dual-slot heat pipe is a promising candidate for the radiator system for the NASA Space Station solar dynamic power modules due to its high thermal transport capability and its potential to be manufactured from any material that comes in tube form. The most difficult machining operation in manufacturing the heat pipes is cutting circumferential grooves on the inside walls of the tube. At present, 10-ft aluminum heat pipe sections have been successfully fabricated using a single point cutting technique. However, a stainless steel heat pipe has been identified as the baseline configuration for the future radiator system and, to date, all attempts at machining stainless steel using single point cutting have produced only limited lengths of satisfactory grooved tubing.

This test consists of two parts. The purpose of the first part is to measure tool life of various single point cutter designs under ideal maching conditions, i.e., cutting grooves on the exterior surface of a tube or bar. The tool design that produces the best results will be used in the second part of the test to measure the effect of different coatings on tool life. The results from both parts of this test will be used to decide if another machining method needs to be investigated.

AUTHORIZATION

This test effort and associated tasks are being performed for the Grumman Space System Division (GSSD) Advanced Thermal Systems group. The work is part of Task Order 2 for Solar Dynamic Heat Rejection Technology, a NASA-Lewis Research Center advanced development contract (NAS3-24665). The Grumman program number associated with this test is 4025-902.

SAFETY PRECAUTIONS

This test will adhere to published Grumman Corporation and machine shop safety precautions.

RESPONSIBILITY

The minimum test criteria indicative of conformance to NASA contract requirements have been determined by the Advanced Thermal Systems group of GSSD.

Conduct of the test, including order of testing, test data reduction, and preparation of the test report, will be the responsibility of the test engineer.

In the event of a test abnormality, the test will stop immediately and the cognizant project engineer will be notified by the test engineer. They will jointly determine the cause of the abnormality, and the project engineer will determine the correct action.

TEST ARTICLES

Single Point Cutters

Part 1 - Three different cutter designs, shown in Fig. 24, will be tested under the same conditions. All of the cutters will be made of C-2 micrograin carbide.

Part 2 - The cutter design that produces the best results in Part 1 will be sent out-of-house to be coated with titanium nitride and Ovonic-47, and then retested.

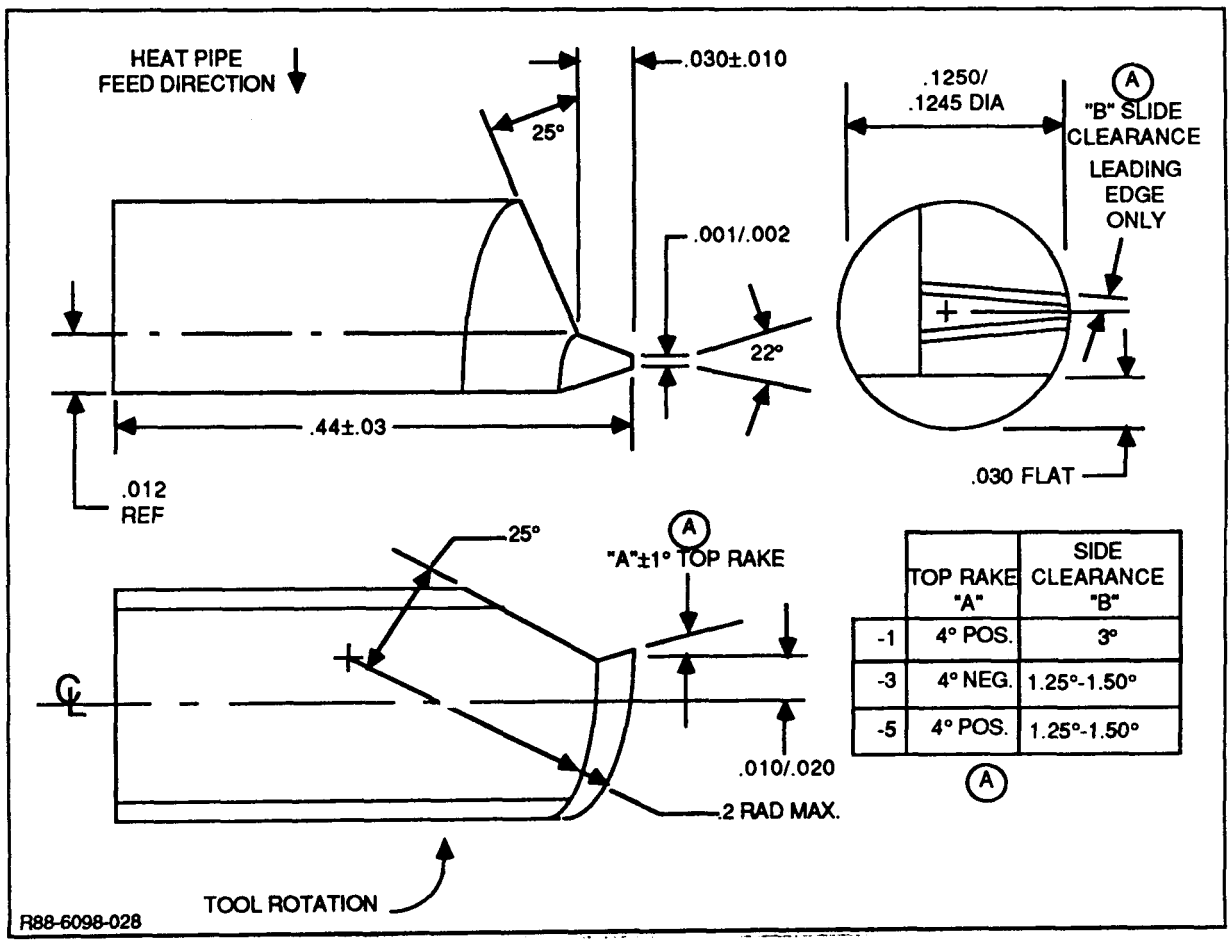

	TOP RAKE "A"	SIDE CLEARANCE "B"
-1	4° POS.	3°
-3	4° NEG.	1.25°-1.50°
-5	4° POS.	1.25°-1.50°

Figure 24 Single Point Cutter Design

Threading Specimens

Parts 1 and 2 - A solid 321 stainless steel bar in the annealed state will be used as the threading specimen. The bar dimensions before test are 2.0-in. diameter x 24.0-in. long. A mild steel bar f similar dimensions will then be used with the coated and uncoated preferred cutter to establish a point of reference.

TEST PARAMETERS

The following test parameters will be covered in the testing of tool life:

Part 1

1. Variation of cutting tool geometries
2. Variation of surface speed of the specimen to be threaded
3. One cut with the optimum cutter design at the optimum speed will be performed on a mild steel bar to establish a point of reference.

Part 2

1. The cutting tool material will not change, but special coatings will be tried to increase tool life for the design that produces the best results
2. Variation of surface speed of the specimen to be threaded
3. One cut with the optimum coated cutter at the optimum speed will be performed on a mild steel bar to establish a point of reference.

EQUIPMENT

The tests will be performed on a conventional engine type lathe capable of cutting 108 threads per inch (TPI). The single point cutting tool is held in place on the carriage of the lathe by a special holder. A drawing of the tool holder is shown in Fig. A-2.

A caliper accurate to within 0.010 in. is used to measure the diameter of the cutting specimen before each test run. A thread comparator is needed to determine the length of a satisfactory cut by locating its boundaries. A satisfactory cut is defined as a trapezoidal groove 0.005 to 0.006-in. deep and 0.002 to 0.003-in. wide.

TEST PREPARATION

Part 1 - Ten tool bits of each design, a total of 30 bits, need to be made to their respective dimension in Fig. 24 before the test. All the cutters will be made of C-2 micrograin carbide. Also, the tool holder will be made to the drawing in Fig. 25.

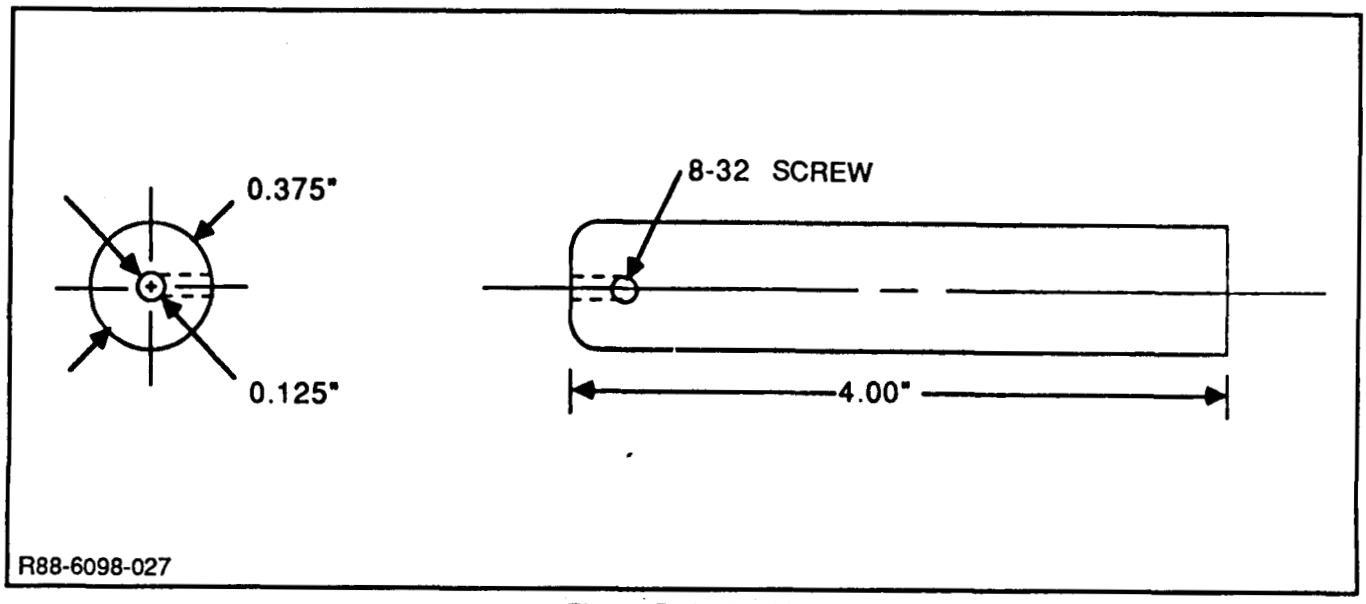

Figure 25 Tool Holder

A water soluble coolant is recommended for cooling the tool bit and removing excess cutting chips. The coolant lines on the lathe should be set up before the test to flood the tool bit at all times during testing.

A mylar drawing of the optimum thread configuration to be used with the optical thread comparator is to be completed before the testing starts.

The stainless steel bar threading specimen is supposed to be fully annealed; thus, the specimen may have to undergo heat treatment prior to the start of testing.

Part 2 - The same procedure as described in Part 1 is to be followed except for the cutter preparation. Twenty tool bits of the design found to be the best in Part 1 need to be made and sent out-of-house to be coated. Half of the cutters (10) is to be coated with titanium nitride; the other half is to be coated with Ovonic-47.

TEST PROCEDURE

Part 1

1. Attach the tool holder to the carriage.
2. Adjust the headstock and tailstock on the lathe to support the threading specimen.
3. Measure and record the outside diameter of the threading specimen.
4. Insert tool bit 1 into the tool holder so that it cuts a 0.006-in. deep groove.

5. Calculate the RPM and feed rate that corresponds to a surface speed of 80 SFM, given the previously measured outside diameter and a constant 108 TPI cut.
6. Make one pass with the cutter along the entire length of the bar at the RPM and feed rate calculated above.
7. Remove the test specimen and check it under an optical thread comparator against the mylar drawing of the optimum thread configuration.
8 Remove the threads just machined with a pass down the bar with a common lathe tool on a different lathe.
9. If the tool bit did not break and produced satisfactory threads along the entire length of the bar stock, repeat steps 2 - 8.
10. If the tool breaks or produces unsatisfactory grooves, repeat steps 2 - 9 with a new tool bit of the same design and a decrease in surface speed of 10 SFM.
11. If the length of cut decreases then increase the surface speed 10 SFM above the starting surface speed and repeat steps 2 - 9.
12 Increment the surface cutting speed by 10 SFM and repeat steps 2 - 9 until an optimum surface speed is attained for the particular tool bit geometry being tested.
13. Repeat steps 2 - 12 with each of the two remaining tool bit designs
14. With the tool bit that produces the longest length of threads, repeat steps 2 - 9 on the mild steel bar at the tool's optimum cutting surface speed.

Part 2

1. Attach the tool holder to the carriage.
2. Adjust the headstock and tailstock on the lathe to support the threading specimen.
3. Measure and record the outside diameter of the threading specimen.
4. Insert the titanium nitride-coated tool bit into the tool holder so that it cuts a 0.006-in. deep groove.
5. Calculate the RPM and feed rate that correspond to the optimum surface speed given the previously measured outside diameter and a constant 108 TPI cut.
6. Make one pass with the cutter along the entire length of the bar at the RPM and feed rate calculated above.

7. Remove the test specimen and check it under an optical thread comparator against the mylar drawing of the optimum thread configuration.
8. Remove the threads just machined with a pass down the bar with a common lathe tool on a different lathe.
9. If the tool bit did not break and produced satisfactory threads along the entire length of the bar stock, repeat steps 2 - 8.
10. If the tool breaks or produces unsatisfactory grooves, repeat steps 2 - 9 with a new tool bit of the same design and a decrease in surface speed of 10 SFM.
11. If the length of cut decreases then increase the surface speed 10 SFM above the starting surface speed and repeat steps 2 - 9.
12. Increment the surface cutting speed by 10 SFM and repeat steps 2 - 9 until an optimum surface speed is attained for the particular tool bit coating being tested.
13. Repeat steps 2 - 12 with the remaining coated tool bit.
14. With the tool bit that produces the longest length of threads, repeat steps 2 - 9 on the mild steel bar at the tool's optimum cutting surface speed.

NASA
National Aeronautics and Space Administration

Report Documentation Page

1. Report No.	2. Government Accession No.	3. Recipient's Catalog No.
NASA CR182141		

4. Title and Subtitle
Solar Dynamic Heat Rejection Technology/Task 2
Final Report/Heat Pipe Radiator Development

5. Report Date
May 1988

6. Performing Organization Code

7. Author(s)
M. League, J. Alario

8. Performing Organization Report No.

10. Work Unit No.
482-56-87

9. Performing Organization Name and Address
Grumman Space Systems Division
111 Stewart Avenue
Bethpage, NY 11714

11. Contract or Grant No.
NAS3-24665

13. Type of Report and Period Covered
Contractor Report
Task 2 Final

12. Sponsoring Agency Name and Address
National Aeronautics and Space Administration
Lewis Research Center
21000 Brook Park Road
Cleveland, OH 44135

14. Sponsoring Agency Code

15. Supplementary Notes
Project Managers, NASA Lewis Research Center: Kerry L. McLallin, Solar Dynamic Power and Propulsion Office
Robert D. Green, Systems Engineering and Integration Division
Grumman Space Systems: Robert H. Haslett
Project Engineer, Grumman Space Systems: Albert W. Carlson

16. Abstract
This report covers the design, fabrication, and test of several dual slot heat pipe engineering development units. This heat pipe design has been identified as a critical component in the development of a high capacity radiator system for the Space Station Solar Dynamic Power System since it can be fabricated from materials other than aluminum (i.e., stainless steel). The following dual-slot heat pipes were fabricated and tested to establish proof of concept: two 6-ft. aluminum heat pipes; a 20-ft. aluminum heat pipe; and a 20-ft. aluminum heat pipe with a four-leg evaporator section. The test results of all four test articles are presented and compared to the performance predicted by the design software. However, test results from the four-leg evaporator test article are incomplete due to difficulties experienced during startup.

The methodology for fabricating stainless steel dual slot heat pipes was also studied by performing a tool life test with different single point cutters, and these results are also presented. Although, the dual-slot heat pipe has demonstrated the potential to meet the requirements for a high capacity radiator system, uncertainties with the design still exist. The startup difficulties with the aluminum test articles must be solved, and a stainless steel/methanol heat pipe should be built and tested before the dual-slot heat pipe can become an acceptable, low-risk design for a wide variety of heat rejection applications.

17. Key Words (Suggested by Author(s))	18. Distribution Statement
Heat Pipe Radiators Heat Pipes Radiator (Thermal) Space Station Solar Dynamic Space Power Station	General Release

19. Security Classif. (of this report)	20. Security Classif. (of this page)	21. No of pages	22. Price*
Unclassified	Unclassified	42	

NASA FORM 1626 OCT 86

*For sale by the National Technical Information Service, Springfield, Virginia 22161